Supporting Information

Nahum et al. 10.1073/pnas.1100296108

SI Methods

Community Model. Within a single population, we track the densities of sensitive cells (S), resistant cells (R), producers (P), and mutant resistant cells (M; we consider only a single mutant class here, but the model easily extends to cover an arbitrary number of mutant classes). Below, we measure density by absorbance in a spectrophotometer, which has a linear relation to cell abundance. For convenience, we refer to the density of the player as well as its type by an italicized capital letter. In the first version of our model, we also track the concentration of nutrients (n). The system is described by the following set of ordinary differential equations (Eqs. S1):

$$\begin{aligned}\dot{S} &= SG_S(n),\\ \dot{R} &= RG_R(n),\\ \dot{P} &= PG_P(n),\\ \dot{M} &= MG_M(n),\\ \dot{n} &= -\varepsilon_S SG_S(n) - \varepsilon_R RG_R(n) - \varepsilon_P PG_P(n)\\ &\quad -\varepsilon_M MG_M(n),\end{aligned} \qquad [S1]$$

where ε_Y is the amount of nutrients needed to shift the absorbance of strain Y by a single unit and $G_Y(n)$ is the growth rate of strain Y. We use a change of variables, where for each player Y (Eq. S2),

$$\varepsilon_Y Y = y, \qquad [S2]$$

such that bacterial density is expressed in terms of nutrient concentration. Thus, we have (Eqs. S3)

$$\begin{aligned}\dot{s} &= sG_S(n),\\ \dot{r} &= rG_R(n),\\ \dot{p} &= pG_P(n),\\ \dot{m} &= mG_M(n),\\ \dot{n} &= -mG_M(n) - sG_S(n) - rG_R(n) - pG_P(n).\end{aligned} \qquad [S3]$$

For convenience, the community is initialized with (Eq. S4)

$$s(0) + r(0) + p(0) + m(0) + n(0) = 1. \qquad [S4]$$

Because (Eq. S5)

$$\frac{d(s+r+p+m+n)}{dt} = 0, \qquad [S5]$$

we know that $s(t) + r(t) + p(t) + m(t) + n(t) = 1$ for all t. Thus, we can rewrite the original system of five differential equations as a system of four (Eqs. S6):

$$\begin{aligned}\dot{s} &= sG_S(1-m-s-r-p),\\ \dot{r} &= rG_R(1-m-s-r-p),\\ \dot{p} &= pG_P(1-m-s-r-p),\\ \dot{m} &= mG_M(1-m-s-r-p).\end{aligned} \qquad [S6]$$

Growth Parameter Estimation. In the previous section, the growth rate (G_Y) of strain Y is a function of limiting nutrient concentration (n). A simple way to assess this function is to measure growth rate at different nutrient concentrations and then fit a curve to yield $G(n)$. Our experiment was conducted in a rich medium (LB); therefore, there was no clear single nutrient to vary. Thus, we took an approximate approach. We substituted fractions of the growth medium (LB) with saline (0.86% NaCl) while maintaining the concentration of tetracycline at a constant level. Each bacterial strain was grown in a microtiter well with 200 μL of a given concentration of impoverished medium for a full 12 h; then, it was diluted fourfold into 200 μL of medium of the same concentration and grown for 1 h. This actively growing bacterial culture was then diluted fourfold into 200 μL of medium of the same concentration and incubated in a spectrophotometer (VersaMax; Molecular Devices). Absorbance (600 nm) was measured at 2-min intervals for 1 h. Let $A_{Y,f}(t)$ be the absorbance of strain Y in impoverished medium with a fraction f of LB (and $1-f$ saline) at time t. Let $G_{Y,f}$ be the slope of the least-squares line $\ln(A_{Y,f}) = G_{Y,f}\,t + b$; thus, $G_{Y,f}$ is the Malthusian growth parameter corresponding to exponential growth. We used the data from time point 1/15 to 7/10 (in hours) to estimate $G_{Y,f}$. For a given strain, we measured $G_{Y,f}$ at a number of different f values (i.e., different concentrations of LB). Using the Monod growth model, we computed the parameters for the least-squares curve (Eq. S7):

$$G_{Y,f} = \frac{\mu_Y f}{\kappa_Y + f}, \qquad [S7]$$

where μ_Y is the maximal growth rate and κ_Y is the fraction of LB necessary to grow at one-half the maximal rate for strain Y. We first determined the least-squares value for μ_S and κ_S. We then used μ_S to constrain the μ_R value ($\mu_R \le \mu_S$) and the least-squares μ_R value to constrain the μ_P value ($\mu_P \le \mu_R$).

Initializing the Metapopulation. Each community's starting spatial layout of the three ancestral strains was determined by running a lattice-based model, in which each lattice point corresponded to one well (subpopulation) within the metapopulation. Using preliminary competition data of the ancestral strains, Fig. S1 shows the number of dilution/growth cycles needed for one strain to displace another.

If we record the state of a well (lattice point) directly after an incubation period, we can describe community dynamics (approximately) by using the following discrete state set: {S, R, P, SR_1, SR_2, SR_3, SR_4, SR_5, RP_1, RP_2, RP_3}. For a well that does not experience an immigration event, the following transitions occur for distinct strains X and Y over a dilution/growth cycle:

$$\begin{aligned}&X \to X,\\ &XY_i \to \begin{cases} X & \text{if } i \text{ is its maximum value,}\\ XY_{i+1} & \text{otherwise.}\end{cases}\end{aligned} \qquad [S8]$$

When migration occurs, the contents of wells in two (potentially different) states are combined. Each entry in Table S1 gives the final state for a well that starts in the row state, is diluted, experiences an immigration event from a well in the column state, and then grows for one period.

The lattice was initialized by randomly assigning each lattice point to the S, R, or P state. At each transfer, each point experienced an immigration event with a probability of 1/3. If an immigration event occurred, a point (representing the source of a migration) within the focal point's neighborhood was chosen at random. Because this simulation emulated the Restricted Community treatment, the neighborhood was restricted to the four nearest lattice points. In the event of migration, the transition

matrix in Table S1 was consulted. If migration did not occur, the transitions outlined in (Eq. **S8**) were followed. The entire lattice was updated synchronously using the previous lattice as a source for all migrations. The resulting arrangement of states after 100 cycles was used to initialize the experimental metapopulations of the Community treatments (using a 12×16 lattice) as well as the Community simulations (using a variety of lattice dimensions).

Calculating the Number of Cell Divisions. We recorded the abundances of cells every $J = 6$ d. Let the number of resistant cells on day t be $R(t)$. Thus, we have recorded $R(Ji)$ for $i \in \{0, 1, 2, 3, \ldots I\}$ (where $I = 6$ is the total number of recorded intervals). For all positive t values less than JI for which we did not record abundance, we linearly interpolate between the nearest known R values to estimate the $R(t)$ value. Thus, given a dilution factor of $\phi = 1/40$, the total number of cell divisions (D) is (Eq. **S9**)

$$D = \sum_{i=0}^{I-1} \left\{ \left(\frac{(J+1) - \phi(J-1)}{2} \right) R(J(i+1)) + \left(\frac{(J-1) - \phi(J+1)}{2} \right) R(Ji) \right\}. \quad \text{[S9]}$$

Additional Resources. All raw data, simulation code, and initialization files can be found at http://depts.washington.edu/kerrpost/Public/RPSProject.

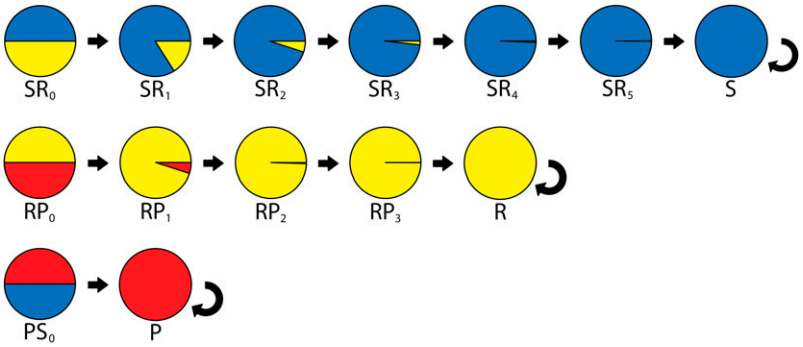

Fig. S1. The frequencies of two competing strains are given as pie charts. Sensitive cells (S; blue) displace resistant cells (R; yellow) over six dilution/growth cycles. Resistant cells displace producers (P; red) over four dilution/growth cycles. Producers kill sensitive cells within a single dilution/growth cycle. The letters and subscripts under each pie chart give each state the name used in the state transition matrix.

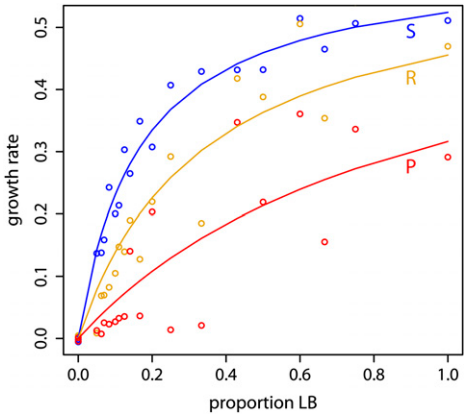

Fig. S2. The growth curves for the three ancestral strains, sensitive (S), resistant (R), and producer (P), are shown. The least-squares parameters for the corresponding Monod functions are given in Table 1. The simulations described in *Methods* used these fitted growth curves.

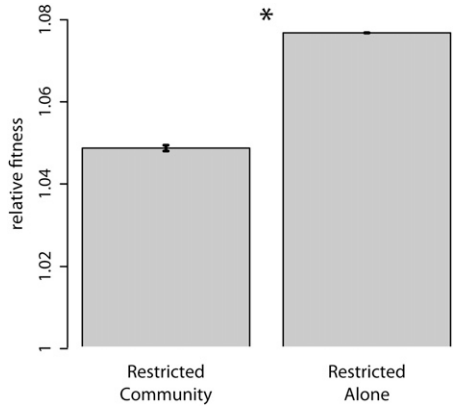

Fig. S3. The average fitness of resistant cells relative to their ancestor after 100 cycles of simulated evolution (as described in the text) in a 100 × 100 lattice. Mean relative fitness of each treatment is shown, and error bars give the SEM. Asterisk indicates a significant difference (Welch's two sample t test; $t_{74.39}$ = 39.44, $P < 0.001$).

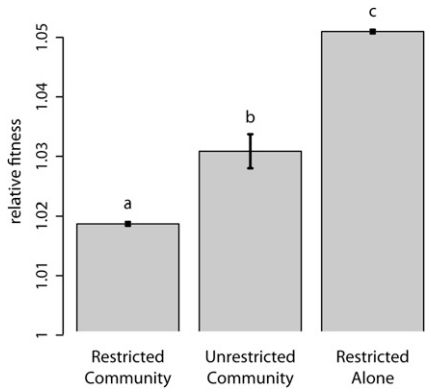

Fig. S4. The average fitness of resistant cells relative to their ancestor after 36 cycles of simulated evolution in a 12 × 16 lattice. Simulation runs in the Unrestricted Community treatment in which the three strains did not coexist were excluded. Mean relative fitness of each treatment is shown, and error bars give the SEM. Letters distinguish treatments significantly different using posthoc comparisons [single-factor ANOVA; $F_{2,2334}$ = 2,329, $P < 0.001$, multiple comparisons by Tukey's Honestly Significant Difference (HSD)].

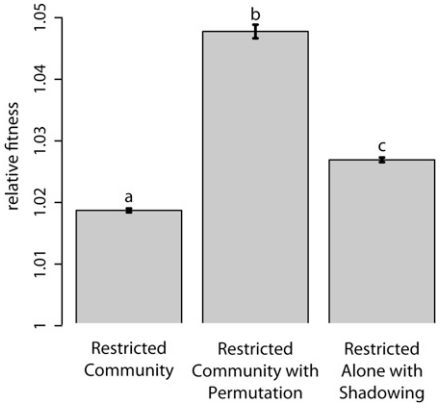

Fig. S5. The average fitness of resistant cells relative to their ancestor after 36 cycles of simulated evolution in a 12 × 16 lattice. Mean relative fitness of each treatment is shown, and error bars give the SEM. Letters distinguish treatments significantly different using posthoc comparisons (single-factor ANOVA; $F_{2,2711}$ = 627.14, $P < 0.001$, multiple comparisons by Tukey's HSD).

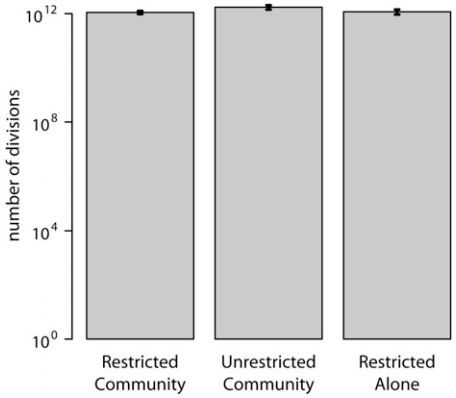

Fig. S6. The number of resistant cell divisions. Mean number of cell divisions in each treatment is shown, and error bars give the SEM. Significant differences among the treatments were not found (single-factor ANOVA; $F_{2,12} = 1.86$, $P = 0.1976$).

Table S1. Transition matrix

	S	R	P	SR_1	SR_2	SR_3	SR_4	SR_5	RP_1	RP_2	RP_3
S	S	SR_1	P	SR_2	SR_3	SR_4	SR_5	S	RP_2	RP_3	R
R	SR_1	R	RP_1	SR_1	SR_1	SR_1	SR_1	SR_1	RP_2	RP_3	R
P	P	RP_1	P	RP_1	RP_1	RP_1	RP_1	RP_1	RP_1	RP_1	RP_1
SR_1	SR_2	SR_1	RP_1	SR_2	SR_2	SR_2	SR_2	SR_2	RP_2	RP_3	R
SR_2	SR_3	SR_1	RP_1	SR_2	SR_3	SR_3	SR_3	SR_3	RP_2	RP_3	R
SR_3	SR_4	SR_1	RP_1	SR_2	SR_3	SR_4	SR_4	SR_4	RP_2	RP_3	R
SR_4	SR_5	SR_1	RP_1	SR_2	SR_3	SR_4	SR_5	SR_5	RP_2	RP_3	R
SR_5	S	SR_1	RP_1	SR_2	SR_3	SR_4	SR_5	S	RP_2	RP_3	R
RP_1	RP_2	RP_2	RP_1	RP_2	RP_2	RP_2	RP_2	RP_2	RP_2	RP_2	RP_2
RP_2	RP_3	RP_3	RP_1	RP_3	RP_3	RP_3	RP_3	RP_3	RP_2	RP_3	RP_3
RP_3	R	R	RP_1	R	R	R	R	R	RP_2	RP_3	R